J. Phys. B: At. Mol. Opt. Phys. 28 (1995) L755–L761. Printed in the UK

LETTER TO THE EDITOR

Experimental observation of the transition from regularity to chaos in diamagnetic Rydberg spectra

N Bouloufa†, P Cacciani†, D Delande‡, C Delsart†, J C Gay‡§, E Luc-Koenig† and J Pinard†

† Laboratoire Aimé Cotton Bat. 505, Campus d'Orsay 91405, Orsay Cedex, France
‡ Laboratoire Kastler-Brossel, Tour 12, Etage 1, 4 place Jussieu, 75005 Paris, France

Received 22 September 1995, in final form 10 November 1995

Abstract. We describe a spectroscopic method and its experimental realization on lithium atoms in a magnetic field which allows a direct observation of the effects of the transition from regularity to chaos in a quantum spectrum by selecting the initial state of the optical excitation. This transition in the classical behaviour is clearly linked to the progressive destruction of some peculiar symmetries of the quantum system.

Until now, to study the quantum counterpart of the transition from regularity to chaos in the classical dynamics of a Hamiltonian system, complex spectra have been analysed through various treatments: statistical distributions of energy level spacings reveal differences between regular and chaotic behaviours [1]; Fourier transforms of scaled energy spectra display peaks at the actions of classical closed orbits whose amplitudes are linked to the stability of the orbits [2, 3].

A more striking quantum manifestation of the classical transition from regularity to chaos has been established theoretically by studying the destruction of the low-field dynamical symmetries of the system [4]. There, it is shown that the destruction of a family of invariant tori in the *classical* phase space is unambiguously linked to the destruction of a corresponding approximate dynamical symmetry for the eigenstates of the *quantum* system. Previous experiments on the Rydberg atoms in a magnetic field [1–3]—a system undergoing a smooth transition from regularity to chaos as the energy is increased—have not been able to observe such an effect. Indeed, optical excitation from an S atomic state is only sensitive to the P component of the excited state. As the total angular momentum is not at all a good quantum number in a strong magnetic field, all the internal dynamical symmetries are simultaneously excited, resulting in spectra with a complexity smoothly increasing with energy. In classical language, the excited electron can explore all the regions of phase space, thus averaging all the local structures. A simple way to overcome this difficulty is to use a *selective excitation* which matches the internal symmetries (phase space structures) of the system.

Here we report experimental results obtained on diamagnetic Rydberg spectra of the lithium atom which demonstrate this effect. Using a specific excitation scheme, the signal reflects the local structure of the classical phase space in a well defined region. Hence, it

§ Deceased.

displays a dramatic change in its complexity at a well defined critical energy—where the classical tori are destroyed. Moreover, this critical energy depends on the region of phase space explored: the same energy spectrum (and eigenstates) can give rise to a clear regular experimental spectrum with one excitation scheme and to a much more intricate one with another excitation scheme.

In a previous paper [5] we have already studied an energy spectrum which reflects the structure of the specific region of phase space around the magnetic field axis. We present here a more extended energy range of this spectrum and we perform a statistical treatment on the intensities of the lines to point out the critical energy. We also present a new spectrum with higher critical energy where an improved resolution is needed, this spectrum reflects the structure of the region of phase space perpendicular to the magnetic field axis.

The Hamiltonian of the hydrogen atom in a magnetic field directed along the z-axis, is (in atomic units):

$$H = \frac{p^2}{2} - \frac{1}{r} + \frac{\gamma}{2}L_z + \frac{\gamma^2}{8}\rho^2 \tag{1}$$

where γ is the magnetic field in units of $B_0 = 2.35 \times 10^5$ T and L_z, the z component of the angular momentum, is a constant.

The classical dynamics of the system only depends on the scaled energy $\varepsilon = E\gamma^{-2/3}$ [6]. At low field strengths ($\varepsilon \ll -1$) two types of regular motion coexist [7]: 'vibrational' localized near the direction of the magnetic field (z-axis) and 'rotational' near the plane perpendicular to the field axis ($z = 0$ plane). Between $\varepsilon = -0.54$ and $\varepsilon = -0.13$, the system smoothly evolves from regularity to complete chaos.

Two simple periodic orbits exist whatever the value of ε: one located on the field axis (limit of the vibrational motion), the other one in the plane perpendicular to the field (limit of the rotational motion). Up to $\varepsilon = -0.13$, the $z = 0$ orbit is stable and surrounded by invariant tori. At the latter value, it becomes unstable and the surrounding tori are destroyed and replaced by a globally chaotic region. The evolution of the orbit along the magnetic field axis is slightly more complicated. At $\varepsilon = -0.39$, a bifurcation takes place: the orbit becomes unstable and a new closed orbit appears, which is stable up to $\varepsilon = -0.30$ where it itself bifurcates [6]. Hence, between -0.39 and -0.30, this orbit is surrounded by invariant tori quite similar to the previous ones. As a rough approximation, the local phase space structure in the vicinity of the orbit along the field can be considered as mainly filled by invariant tori up to $\varepsilon = -0.30$, and mainly chaotic above.

In a quantum approach, when the diamagnetic terms is small compared to the Coulomb one, the natural basis to be used is the spherical one. In this regime, the diamagnetic interaction removes the degeneracy in the Rydberg n-shell leading to the diamagnetic manifold [8]. Two different limiting symmetries coexist in this manifold. In the lower part, the states are well described in terms of the parabolic basis (n, n_1, M) eigenfunctions of the A_z component of the Runge–Lenz vector: the lowest component of each diamagnetic manifold is almost a pure $n_1 = 0$ state (overlap $\approx 85\%$). In the upper part of the manifold, the states are well described by the 'lambda' basis (n, λ, M), eigenfunctions of the square of the angular momentum Λ (A_x, A_y, L_z) where A is the Runge–Lenz vector: the highest component of each diamagnetic manifold is almost a pure $\lambda = n - 1$ state (overlap $\approx 98\%$). In this low-field regular regime, the eigenstates are localized on the classical invariant tori [9]. The parabolic states are localized on the vibrational tori surrounding the orbit along the field while the 'lambda' states are localized on the rotational tori surrounding the $z = 0$ orbit [4].

At higher energy, the introduction of the Coulomb dynamical group $SO(2, 2)$ allows us to build a suitable Sturmian basis. Two bases are of special interest: the parabolic basis and λ type basis which generalize those known within an n Rydberg shell. By projecting all the eigenstates on the extreme parabolic or λ subspaces, Delande and Gay [4] have analysed the destruction of the parabolic and λ symmetries with increasing energy. Two synthetic spectra representing $\sum_n |\langle\psi_f|\phi_n\rangle|^2$ versus energy are drawn in figure 1, where ϕ_n is either $(n, n_1 = 0, M = 0)$ or $(n, \lambda = n-1, M = 0)$ and ψ_f the final states. In the weak-field limit (left-hand part of each spectrum) the spectrum is very sparse, almost composed of only one component per manifold corresponding to the lowest or the highest state. At higher energy corresponding to the critical ε value, the studied dynamical symmetry is destroyed and the intensity is spread over several energy levels, consequently a high density of excitation lines burst out. These quantum critical values are very close to the classical ones (the arrows on the figures) where the local structures of phase space around the parallel and perpendicular orbits turn from regular to chaotic. Hence, the manifestation of *classical* chaos appears as the destruction of the dynamical symmetries identified in the weak-field *quantum* spectra.

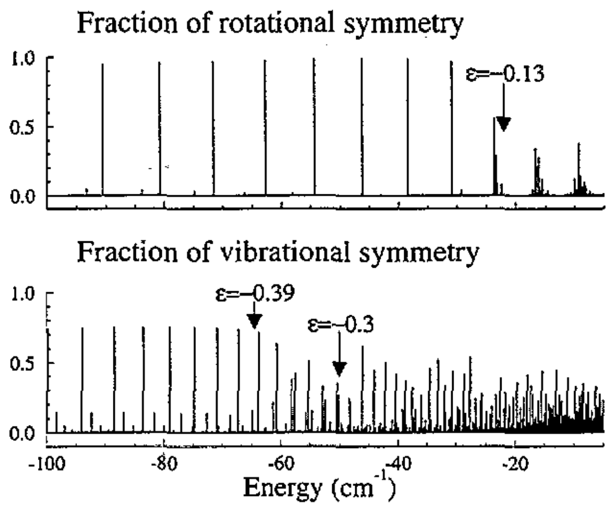

Figure 1. Squared projections of the even parity eigenstates of the hydrogen atom in a magnetic field of 4.9 T (*a*) on the subspace $(n, n_1 = 0, M = 0)$ (*b*) on the subspace $(n, \lambda = n-1, M = 0)$. The arrows indicate the transition to chaos in the corresponding regions of the classical phase space. For the vibrational symmetry, the first arrow (−0.39) indicates the destabilization of the orbit along the field while the second arrow (−0.30) is the onset of full chaos in its vicinity.

The basis of our experimental method is to choose an initial state with a well defined symmetry (the upper or the lower state of a diamagnetic manifold). Calculations have shown that the electric dipolar excitation approximately preserve the diamagnetic symmetries: starting from a state of well defined dynamical symmetry, final states of the same symmetry are excited preferably. As a result, the ideal projections proposed before can be nearly made experimentally: the excitation spectrum is simple and less dense in the regular region and the modification due to the onset of chaos is more striking. Classically, by choosing the starting state as a diamagnetic one, a well defined angle of the electron momentum with respect to the magnetic field is selected at the nucleus. As this angle is nearly kept constant during the excitation, in the phase space we only explore the vicinity of the trajectory with this initial condition.

The experiment was performed on the lithium atom. The initial state of the final transition is chosen as a state of the $n = 10$ diamagnetic manifold. Due to core effects, an efficient excitation of the diamagnetic components of interest on the $n = 10$ manifold can only be obtained in a two-step excitation and if the 10d excited state is mixed with the other components of this manifold. This can be done using the Stark switching method: an additional electric field of 200 V cm^{-1} is superimposed to the magnetic field, this field is switched to zero before performing the last excitation.

The experiment has been described in a previous paper [5] and we just focus on its specific aspects. A highly collimated atomic beam of lithium travelling parallel to the magnetic field is excited perpendicularly to high Rydberg states by a three-step excitation: the first laser is a continuous extended cavity diode laser at 670 nm servolocked on the fluorescence signal. The second one is a single-mode continuously tunable pulsed dye laser system [10] doubled in a non-linear crystal to obtain the wavelength of 360 nm necessary to reach the chosen $n = 10$ diamagnetic component. It is stabilized using a sigmameter [11] which ensures good long term stability. The third stage uses an identical dye laser system which provides up to 50 mJ at 750 nm, this beam is focused in a Raman cell filled with 15 bars of H_2 in order to generate light in the 9–10 μm range through stimulated third Stokes Raman scattering. The use of a capillary increases the efficiency and up to 10 μJ was obtained. The spectral resolution is limited by pressure broadening, it is about 1 GHz FWHM. This IR generating process was used in the experiment which allowed us to study the destruction of the parabolic symmetry. In the case of the λ symmetry whose destruction is predicted at higher energy where the spectrum is more dense, better spectral resolution is needed. For this reason, the last excitation stage has been modified. Instead of Raman shifting process, we have developed difference frequency mixing of two red pulses in a non-linear optical crystal of $AgGaS_2$ to obtain an infrared radiation with a linewidth of 100 MHz.

High-resolution analysis of the paramagnetic splitting of the 2p state allows us to determine the value of the magnetic field strength with a relative uncertainty of 10^{-3}.

To optimize the selectivity the choice of the three laser polarizations is done by looking at the calculated spectrum for the $n = 22$ diamagnetic manifold. The polarization scheme σ^+, π, π (resp. $\sigma^+, \sigma^-, \sigma$) is designed to simulate the projection scheme on the parabolic (resp. λ) basis mentioned above.

Figure 2 shows the spectrum recorded from -80 cm^{-1} to -17 cm^{-1} starting from the lowest odd parity parabolic component of the ($n = 10$, $M = 1$) manifold at a magnetic field of 4.9 T ($\gamma = 2.091 \times 10^{-5}$). The simulated spectrum is drawn under the experimental one, energies and wavefunctions of the final even states are calculated in the pure hydrogen case (the quantum defect of the d state is neglected) by diagonalization in a Sturmian basis [12]. The agreement between the calculated and the experimental spectra is impressive concerning the positions of lines. The discrepancy in the intensity ratio between strong and small lines can be attributed to saturation phenomena; the general broadening of the strong lines confirms this interpretation.

The first part of these calculated and experimental spectra is more complicated than the synthetic one (figure 1) because even in the low-field regime, at least the two lowest components of each manifold have a significant excitation probability. Nevertheless, the change in the spectrum corresponding to the onset of chaos is observable experimentally: in the first part the spectrum is sparse, structured in two or three series, in the second one the density of significantly excited lines increases rapidly making impossible the identification of the lines.

In a more quantitative way, the statistical distribution of the line intensities within a

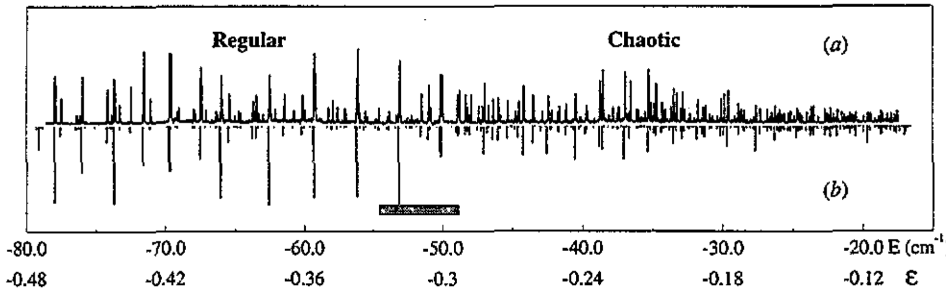

Figure 2. Recording of the vibrational, $M = +1$, even-parity spectrum in a magnetic field of 4.9 T (*a*) experiment on lithium, (*b*) numerical simulation on hydrogen. The shaded rectangle marks the transition region from regularity to chaos, around $\varepsilon = -0.31$.

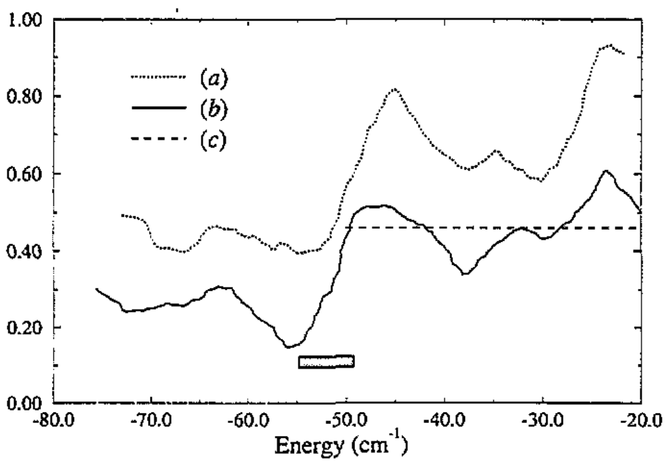

Figure 3. Fraction of the lines per 6 cm^{-1} whose intensity is greater than half the mean intensity value deduced (*a*) from the experimental spectrum, (*b*) from the calculated one, (*c*) from the Porter–Thomas distribution (prediction of the random matrix theory). The shaded rectangle marks the transition region from regularity to chaos, around $\varepsilon = -0.31$.

given range can be studied. In figure 3, we plot the result of a treatment performed on both experimental (*a*) and calculated (*b*) spectra: for a given energy the lines within a constant range (6 cm^{-1}) are measured, the mean intensity I_{mean} is calculated and we measure the fraction of those whose intensity is greater than $0.5 \times I_{\text{mean}}$. Curve (*a*) lies above curve (*b*) because in the experimental spectrum, the noise does not allow one to see the smallest lines present in the calculated spectrum. The two curves display a sharp step at an ε value very closed to that where the local structure of the phase space becomes mainly chaotic ($\varepsilon = -0.3$, $E = -50$ cm^{-1}).

Above this value, in the chaotic domain [-50 cm^{-1}, -17 cm^{-1}], the statistical distribution of the intensities has been studied and compared successfully with a Porter Thomas distribution [13], the one predicted for a chaotic system by the random matrix theory [9]. The broken line (*c*) drawn above -50 cm^{-1} in figure 3 is the value deduced from this model.

We also studied the destruction of the λ symmetry. A σ polarization is needed for the last laser stage and two identical spectra ($M = \pm 1$) shifted by the paramagnetic term are excited. This increases the number of lines and the difficulties of interpretation. In addition the intensity of the lines of interest is an order of magnitude smaller in this experiment than in the parabolic case.

Figure 4 shows the spectrum recorded from -42 cm^{-1} to -12 cm^{-1} starting from the highest even-parity λ component of the ($n = 10$, $M = 0$) manifold at a magnetic field of 4.87 T ($\gamma = 2.071 \times 10^{-5}$). The simulated spectrum is drawn under the experimental one. The calculation has been carried out taking into account the quantum defects of the lithium atom on both starting and final states [12]. The positions of the lines are well reproduced but the intensities show more pronounced discrepancies than in the parabolic case. This is probably due to the reliability of the IR laser power which is sensitive to the angular phase matching of the non-linear crystal. The transition from regularity to chaos is more difficult to see because of the superposition of the two shifted identical spectra. Therefore one of its characteristic feature can be followed focusing on the $M = -1$ spectrum: transition from a series of isolated lines (stars) to bunches of lines (braces) across the value $\varepsilon = -0.13$ (see also figure 1).

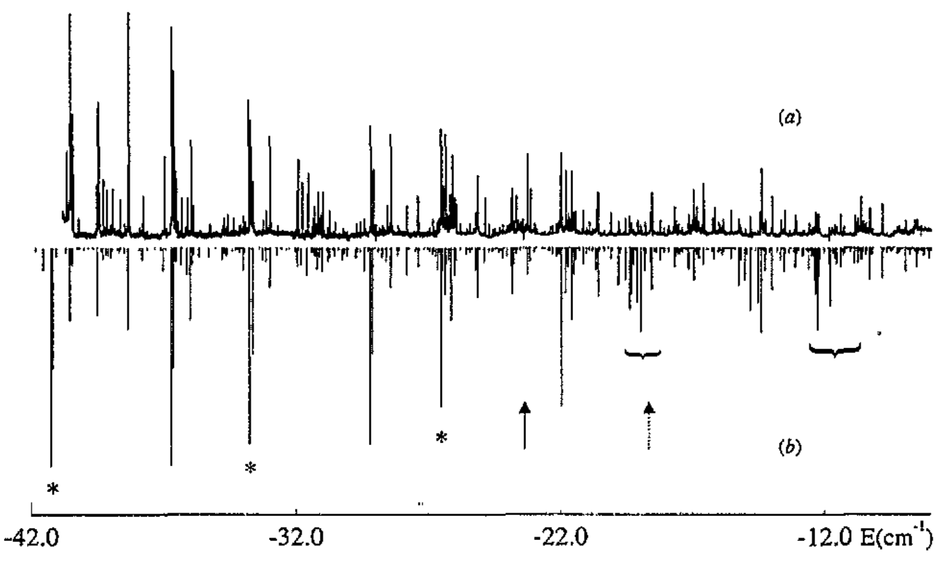

Figure 4. Recording of the rotational, $M = \pm 1$, odd parity spectrum in a magnetic field of 4.87 T (*a*) experiment, (*b*) simulation $M = -1$ (full lines) and $M = +1$ (broken lines). The arrows indicate the onset of classical chaos in the vicinity of the $z = 0$ orbit for $M = -1$ and $M = +1$ cases. Stars and braces: see the text.

Although these two spectra (figures 2 and 4) involve the same states $|M| = 1$ (except for parity), they show a fundamental difference in the energy range [-42 cm^{-1}, -21 cm^{-1}] which is seen as regular or chaotic depending on the excitation scheme or, in classical language, depending on the part of the phase space probed.

To our knowledge, this is the first time that a signature of the classical transition from regularity to chaos has been directly observed in experimental spectra of an atom in a magnetic field.

Thanks to a selective excitation, it was possible to clarify the spectrum by only populating final states with a well defined symmetry. The onset of chaos manifests as the destruction of this symmetry and the spread of oscillator strength over neighbouring levels. For each of the two symmetries typical of diamagnetism, the critical energy has been determined directly and agrees very well with the values obtained from a classical analysis of the system.

References

[1] Welch G R, Kash M M, Iu C, Hsu L and Kleppner D 1989 *Phys. Rev. Lett.* **62** 893
[2] Van Der Veldt T, Vassen W and Hogervost W 1993 *Europhys. Lett.* **21** 903
[3] Holle A, Main J, Wiebush G, Rottke H and Welge K H 1986 *Phys. Rev. Lett.* **57** 3261
[4] Delande D and Gay J C 1987 *Phys. Rev. Lett.* **59** 1809
[5] Bouloufa N, Cacciani P, Delande D, Delsart C, Gay J C, Luc-Koenig E and Pinard J 1992 *J. Physique II* **2** 671
[6] Friedrich H and Wintgen D 1989 *Phys. Rep.* **183** 37
[7] Solov'ev E A 1981 *Sov. Phys.–JETP* **34** 265
[8] Cacciani P, Luc-Koenig E, Pinard J, Thomas C and Liberman S 1986 *Phys. Rev. Lett.* **56** 1124
[9] Giannoni M J, Voros A and Zinn-Justin J (eds) 1991 *Chaos and Quantum Physics Proc. Les Houches Summer School* Session LII (Amsterdam: North-Holland)
[10] Pinard J and Liberman S 1977 *Opt. Commun.* **20** 344
[11] Juncar P and Pinard J 1975 *Opt. Commun.* **14** 438
[12] Halley M H, Delande D and Taylor K T 1993 *J. Phys. B: At. Mol. Opt. Phys.* **26** 1775
[13] Hasegawa H, Robnik M and Wunner G W 1989 *Rep. Prog. Theor. Phys.* **98** 198